may be achieved by repetitive induction of LTP or LTD that counteracts the reversal action of spontaneous activity. We hypothesized that, whereas one episode of induction stimuli fails to induce persistent synaptic modifications, repetition of induction episodes in a "spaced" manner might result in persistent synaptic modifications, and the extent of stable modification might depend on the spacing of the induction episodes (Fig. 4A). We tested this hypothesis on TBS-induced LTP at retinotectal synapses. The magnitude of LTP is saturated when the total number of bursts in the TBS exceeded 20. However, synaptic potentiation induced by TBS (60 bursts) was completely abolished by 20 min of spontaneous activity (in c.c.), interrupted briefly three times for monitoring of EPSCs, after the induction of LTP (Fig. 4B). This reversal of synaptic potentiation was not due to deleterious neuronal or synaptic conditions, because subsequent TBS (20 bursts) was fully effective in inducing LTP to a similar extent (Fig. 4B). In contrast to the "massed" TBS (60 bursts) in one induction episode, spaced application of three episodes of TBS (20 bursts each) within the 20-min period counteracted the effect of spontaneous activity, resulting in persistent synaptic potentiation. Residual potentiation resulting from each TBS episode accumulated when the subsequent TBS episode was applied before the reversal was completed (Fig. 4C) (*11*). Spaced TBS was effective in producing stable LTP, to a level that occluded further potentiation by subsequent TBS application (Fig. 4D). Furthermore, when the interval between TBS episodes increased beyond an optimal interval of 5 min, the extent of stabilization became progressively diminished (Fig. 4E). Finally, we tested whether moving-bar stimulation with a spaced rather than a massed pattern could lead to the long-lasting appearance of directional sensitivity in tectal neurons (*11*). Preference toward the trained direction was found in 12 out of 25 tectal neurons that were trained with the spaced pattern, whereas no preference was observed in 15 out of 15 cells that were trained with the massed pattern of stimuli (Fig. 4F).

Our results demonstrate the disruptive influence of spontaneous activity on experience-induced synaptic modifications in vivo and suggest the existence of a temporal constraint on the pattern of visual inputs necessary for induction of stable synaptic modifications. Because the developing visual system is highly modifiable by light exposure (*13*, *14*, *31*), the susceptibility of synaptic modification to reversal by spontaneous activity may serve as a protective mechanism against long-lasting synaptic changes triggered by incidental episodes of correlated activity. In the face of this susceptibility, a spaced pattern of visual inputs becomes essential for stable synaptic modifications.

References and Notes

1. D. H. Hubel, T. N. Wiesel, *J. Neurophysiol.* **28**, 1041 (1965).
2. T. N. Wiesel, *Nature* **299**, 583 (1982).
3. L. C. Katz, C. J. Shatz, *Science* **274**, 1133 (1996).
4. A. A. Penn, C. J. Shatz, *Pediatr. Res.* **45**, 447 (1999).
5. L. I. Zhang, M. M. Poo, *Nature Neurosci.* **4** (suppl.), 1207 (2001).
6. T. V. Bliss, G. L. Collingridge, *Nature* **361**, 31 (1993).
7. S. J. Martin, P. D. Grimwood, R. G. Morris, *Annu. Rev. Neurosci.* **23**, 649 (2000).
8. E. R. Kandel, *Science* **294**, 1030 (2001).
9. Y. Dudai, *Curr. Opin. Neurobiol.* **12**, 211 (2002).
10. Nieuwkoop and Faber (*32*) stage 43 to 46 *Xenopus laevis* tadpoles were anesthetized with saline that contained 0.02% 3-aminobenzoic acid ethyl ester secured by insect pins to a sylgard-coated dish, and incubated in Hepes-buffered saline that contained 115 mM NaCl, 2 mM KCl, 10 mM Hepes, 3 mM $CaCl_2$, 10 mM glucose, 1.5 mM $MgCl_2$, and 0.005 mM glycine (pH 7.4). For recording, the skin was removed and the brain was split open along the midline to expose the inner surface of the tectum. A low dose of α-bungarotoxin (1 μg/ml) was applied to the bath to prevent muscle contraction. As previously shown (*12*), this toxin treatment did not significantly affect the retinotectal responses.
11. Materials and methods are available as supporting material on *Science* Online.
12. L. I. Zhang, H. W. Tao, C. E. Holt, W. A. Harris, M. M. Poo, *Nature* **395**, 37 (1998).
13. L. I. Zhang, H. Tao, M. Poo, *Nature Neurosci.* **3**, 708 (2000).
14. H. W. Tao, L. I. Zhang, F. Engert, M. Poo, *Neuron* **31**, 569 (2001).
15. S. B. Udin, S. Grant, *Prog. Neurobiol.* **59**, 81 (1999).
16. M. Weliky, L. C. Katz, *Science* **285**, 599 (1999).
17. The reversal of LTP is not due to a decline in the quality of the recording, because LTP of a similar magnitude can be induced after the reversal (n = 4 cells) (Fig. 4B).
18. For TBS, inputs were stimulated for 20 bursts at 5 Hz, with each burst containing 5 pulses at 200 Hz.
19. F. Engert, H. W. Tao, L. I. Zhang, M. Poo, *Nature* **419**, 470 (2002).
20. Whether an RGC input underwent potentiation or depression after moving-bar stimulation did not depend on the initial strength of that input. Both potentiation and depression were frequently observed at two independent RGC inputs onto the same tectal neuron after moving-bar training.
21. Q. Zhou, H. W. Tao, M.-m. Poo, data not shown.
22. D-APV infusion in this tectum preparation effectively abolished the NMDA receptor component of EPSCs at the retinotectal synapses, without significantly affecting synaptic currents and spiking activity induced by light exposure (*12*, *13*).
23. J. Larson, P. Xiao, G. Lynch, *Brain Res.* **600**, 97 (1993).
24. U. Staubli, D. Chun, *J. Neurosci.* **16**, 853 (1996).
25. S. M. Dudek, M. F. Bear, *J. Neurosci.* **13**, 2910 (1993).
26. H. K. Lee, M. Barbarosie, K. Kameyama, M. F. Bear, R. L. Huganir, *Nature* **405**, 955 (2000).
27. L. Xu, R. Anwyl, M. J. Rowan, *Nature* **394**, 891 (1998).
28. T. J. O'Dell, E. R. Kandel, *Learn. Mem.* **1**, 129 (1994).
29. S. Fujii, K. Saito, H. Miyakawa, K. Ito, H. Kato, *Brain Res.* **555**, 112 (1991).
30. C. C. Huang, Y. C. Liang, K. S. Hsu, *J. Neurosci.* **19**, 9728 (1999).
31. W. C. Sin, K. Hass, E. S. Ruthszer, H. T. Cline, *Nature* **419**, 475 (2002).
32. P. D. Nieuwkoop, J. Faber, *Normal Table of* Xenopus laevis (North Holland, Amsterdam, ed. 2, 1967).

33. Supported by grants from NSF (grant no. IBN-0196100) and NIH (grant no. NS 36999) (M.-m.P.) and by a National Research Service Award (Q.Z.).

Supporting Online Material

www.sciencemag.org/cgi/content/full/300/5627/1953/DC1
Materials and Methods
Fig. S1

9 January 2003; accepted 30 April 2003

Translation of Polarity Cues into Asymmetric Spindle Positioning in *Caenorhabditis elegans* Embryos

Kelly Colombo,[1] Stephan W. Grill,[2] Randall J. Kimple,[3] Francis S. Willard,[3] David P. Siderovski,[3] Pierre Gönczy[1]*

Asymmetric divisions are crucial for generating cell diversity; they rely on coupling between polarity cues and spindle positioning, but how this coupling is achieved is poorly understood. In one-cell stage *Caenorhabditis elegans* embryos, polarity cues set by the PAR proteins mediate asymmetric spindle positioning by governing an imbalance of net pulling forces acting on spindle poles. We found that the GoLoco-containing proteins GPR-1 and GPR-2, as well as the Gα subunits GOA-1 and GPA-16, were essential for generation of proper pulling forces. GPR-1/2 interacted with guanosine diphosphate-bound GOA-1 and were enriched on the posterior cortex in a *par-3*– and *par-2*–dependent manner. Thus, the extent of net pulling forces may depend on cortical Gα activity, which is regulated by anterior-posterior polarity cues through GPR-1/2.

The mechanisms that establish cell polarity are increasingly well understood, but relatively little is known about how polarity cues are translated into appropriate spindle positioning (*1, 2*). The PAR proteins, which are essential for cell polarity across metazoan evolution (*3*), were originally identified in the nematode *C. elegans* (*4*), where they establish polarity along the anterior-posterior (AP) axis after fertilization. During mitosis in one-cell stage *C. elegans* embryos, PAR proteins govern an imbalance of forces acting along astral microtubules and pulling on spindle poles (*5*). As a larger net force pulls on the posterior spindle pole, the spindle elongates asymmetrically and the first division is unequal. The components required for the generation of pulling forces have not yet been

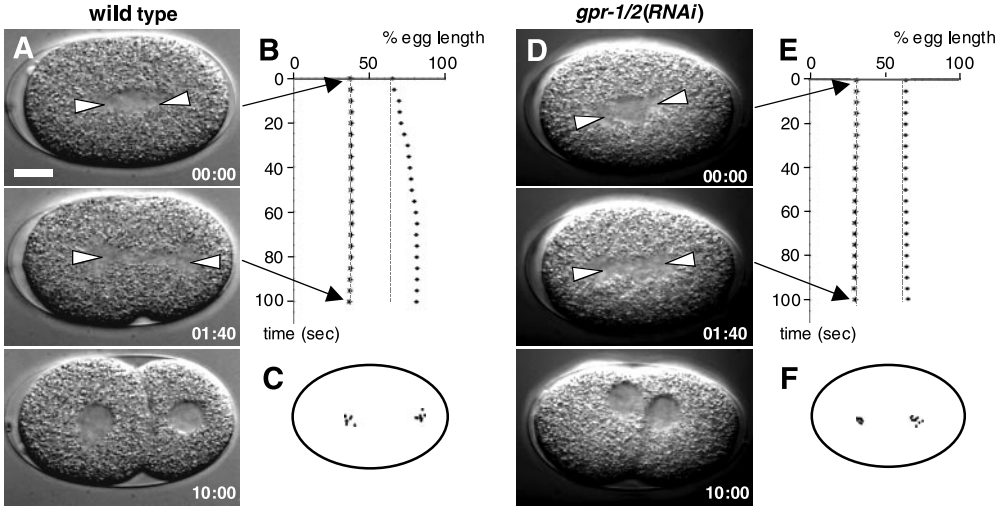

Fig. 1. GPR-1/2 are required for asymmetric spindle positioning. (**A** and **D**) Time-lapse DIC microscopy of wild-type (A) and *gpr-1/2*(*RNAi*) (D) one-cell stage embryos. In this and other figures, anterior (0% egg length) is to the left; arrowheads point to spindle poles. Time elapsed is shown in minutes and seconds. Panels in (A) and (D) are at same magnification; scale bar, 10 μm. (**B** and **E**) Tracings of anterior and posterior spindle pole position of wild-type (B) and *gpr-1/2*(*RNAi*) (E) embryo displayed in (A) and (D), from spindle assembly until 100 s thereafter. Vertical dashed lines indicate starting positions of spindle poles. (**C** and **F**) Position of anterior and posterior spindle poles at the end of anaphase in 9 wild-type embryos (C) and 10 *gpr-1/2*(*RNAi*) embryos (F).

established, nor has the mechanism by which AP polarity is translated into differential net forces exerted on the two spindle poles.

Simultaneous inactivation of the genes encoding Gα subunits GOA-1 and GPA-16 in one-cell stage *C. elegans* embryos causes an equal first division with no apparent polarity defects (*6*), which indicates that Gα signaling is required downstream of the PAR proteins or in a parallel pathway to mediate proper spindle positioning. Such a role may be evolutionarily conserved. While *Drosophila* $G\alpha_i$ and the interacting GoLoco ($G\alpha_{i/o}$-Loco)–containing protein Pins play a role in maintaining polarity cues (*7*–*9*), they also function in conjunction with the PAR-3 ortholog Bazooka and associated components to direct spindle positioning (*10*). The nature of the forces governing asymmetric spindle positioning has not been investigated in *Drosophila*, precluding analysis of the consequences of Gα inactivation at the biophysical level.

We performed an RNA interference (RNAi)–based functional genomic screen to identify cell division components in *C. elegans* (*11*) and uncovered two genes, *gpr-1* and *gpr-2* (G protein regulator), whose inactivation caused a striking spindle-positioning defect in one-cell stage embryos. Because *gpr-1* and *gpr-2* are >97% identical at the nucleotide level (*12*), they are likely both silenced when either gene is targeted by RNAi, as is the case for other gene pairs so closely related (*13*). *gpr-1* and *gpr-2* encode essentially identical 525–amino acid proteins harboring a coiled-coil domain (residues 186 to 213) and a GoLoco motif (residues 425 to 445).

[1]Swiss Institute for Experimental Cancer Research (ISREC), 1066 Epalinges/Lausanne, Switzerland. [2]Max Planck Institute of Molecular Cell Biology and Genetics, 01307 Dresden, Germany. [3]Department of Pharmacology, University of North Carolina at Chapel Hill, Chapel Hill, NC 27599, USA.

*To whom correspondence should be addressed. E-mail: pierre.gonczy@isrec.unil.ch

In wild-type one-cell stage embryos (Fig. 1, A to C) (movie S1), the spindle elongates asymmetrically toward the posterior during anaphase, accompanied by vigorous transverse movements of the posterior spindle pole, which flattens at telophase. As a result, the first division is unequal, generating a larger anterior blastomere and a smaller posterior one. In *gpr-1/2*(*RNAi*) one-cell stage embryos (Fig. 1, D to F) (movie S2), the spindle did not elongate asymmetrically during anaphase in 25 of 30 cases. As a result, the first division was equal, generating two blastomeres of identical size. In the other five *gpr-1/2*(*RNAi*) embryos, the posterior spindle pole underwent weak posterior displacement, which, although clearly distinguishable from the wild type, resulted in unequal first division (*14*). In all *gpr-1/2*(*RNAi*) embryos, transverse movements of the posterior spindle pole and its flattening at telophase did not take place. Other defects were apparent when *gpr-1* and *gpr-2* were inactivated by RNAi, including aberrant centrosome and spindle positioning in two-cell stage embryos as well as occasional chromosome segregation defects (movie S2).

To determine whether the lack of posterior spindle displacement in one-cell stage *gpr-1/2*(*RNAi*) embryos resulted from defective AP polarity cues, we examined the distribution of PAR-6, PAR-3, PAR-2, and PAR-1, which are asymmetrically distributed along the AP axis in the wild type (*15*–*18*). We found that all four PAR proteins were correctly distributed in *gpr-1/2*(*RNAi*) embryos (fig. S1). Moreover, the distribution of P granule ribonucleoproteins and of the germline protein PIE-1, which are restricted to the posterior of wild-type one-cell stage embryos in response to polarity cues (*19, 20*), was not altered (fig. S1) (*14*). Thus, lack of posterior displacement in *gpr-1/2*(*RNAi*) embryos was not due to defective AP polarity, and GPR-1/2 act downstream of the PAR proteins or in a parallel pathway to mediate proper spindle positioning.

Because the phenotype of *gpr-1/2*(*RNAi*) embryos is indistinguishable from that of *goa-1*/*gpa-16*(*RNAi*) embryos (*6*), and because other GoLoco-containing proteins regulate $G\alpha_i$ or $G\alpha_o$ activity (*21*–*23*), we reasoned that GPR-1/2 may be required for Gα signaling in *C. elegans* embryos. Consistent with this view, simultaneous depletion of *gpr-1*, *gpr-2*, *goa-1*, and *gpa-16* did not result in more severe phenotypic manifestations (*14*). Furthermore, as for *goa-1*/*gpa-16*(*RNAi*) embryos (*6*), inactivation of the Gβ subunit *gpb-1* or of the Gγ subunit *gpc-2* did not rescue the phenotype of one-cell stage *gpr-1/2*(*RNAi*) embryos (*14*), which demonstrates that the spindle-positioning defect is not caused by excess Gβ/Gγ activity.

We investigated whether GPR-1/2 physically interact with GOA-1 and/or GPA-16. Using a yeast two-hybrid assay, we detected an interaction with GOA-1 but not with GPA-16 (Fig. 2A). Similarly, glutathione *S*-transferase (GST)–GPR-1 bound to GOA-1 in a GST pull-down assay (Fig. 2B) but did not exhibit interaction above background with GPA-16 (*14*). The lack of detectable interaction between GPR-1 and GPA-16 in these assays may reflect weaker binding affinity. We used the GST pull-down assay to map the domain of GPR-1 that mediates interaction with GOA-1, and found it to reside within the C-terminal–most 185 amino acids (Fig. 2B). The GoLoco motif contained in this fragment, which is identical in GPR-1 and GPR-2, was sufficient for interaction (Fig. 2B).

To investigate the nucleotide dependence of this interaction, we used a surface plasmon resonance (SPR) binding assay to test the ability of GOA-1 to bind to GST–GPR-1. Before injection over SPR surfaces, recombinant GOA-1 was first incubated with GTP-γ-S [guanosine 5′-*O*-(3′-thiotriphosphate)], with guanosine diphosphate (GDP)–AlF_4^- to

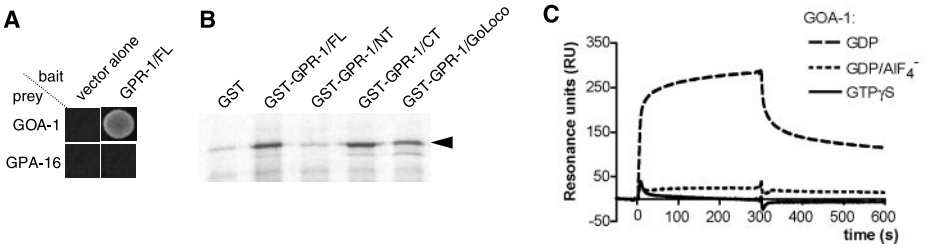

Fig. 2. GPR-1/2 interact with GOA-1–GDP through the GoLoco motif. (**A**) Two-hybrid experiment using a histidine reporter to test interaction between full-length GPR-1 and GOA-1 or GPA-16; plate contains 50 mM 3-aminotriazol. (**B**) GST pull-down experiment with in vitro translated [^{35}S]GOA-1 (arrowhead) and GST fused to full-length GPR-1 (GST–GPR-1/FL) or fragments thereof (GST–GPR-1/NT, residues 1 to 340; GST–GPR-1/CT, residues 341 to 525; GST–GPR-1/GoLoco, residues 425 to 445). Quantification of two experiments (including the one shown) indicates the following average increases in radioactive material pulled down over GST alone: GST–GPR-1/FL, 18.6 (SD = 2.6); GST–GPR-1/NT, 1.8 (SD = 1.1); GST–GPR-1/CT, 14.0 (SD = 4.0); GST–GPR-1/GoLoco, 7.0 (SD = 1.9). GST–GPR-1/FL pulled down ~10% of input material (*14*). (**C**) SPR binding assay testing nucleotide dependence of interaction between GOA-1 and GST–GPR-1/GoLoco; the *y* axis indicates specific binding (in relative resonance units) as subtracted from background binding to GST alone.

mimic the transition state of GTP hydrolysis, or with GDP alone. The GoLoco motif of GPR-1 bound robustly to GOA-1–GDP (binding affinity K_d = 0.31 μM, χ^2 = 44.3) but exhibited no binding to GTP-γ-S–bound or AlF_4^--activated GOA-1 (Fig. 2C) (fig. S2). Similar results were obtained with the C-terminal–most 185 amino acids of GPR-1 (fig. S2). By analogy with other GoLoco-containing proteins that specifically interact with GDP-bound Gα subunits (*21–23*), GPR-1/2 likely function as guanine nucleotide dissociation inhibitors. Because the loss of GPR-1/2 caused a phenotype indistinguishable from that of GOA-1 and GPA-16, it appears that the GDP-bound form of Gα subunits, rather than the GTP-bound form, mediates spindle positioning in one-cell stage *C. elegans* embryos.

We next used in vivo spindle-severing experiments to investigate the extent of astral pulling forces in the absence of *gpr-1* and *gpr-2* or of *goa-1* and *gpa-16*. We cut the spindle with a localized ultraviolet laser microbeam and monitored the behavior of spindle poles with the use of time-lapse differential interference contrast (DIC) microscopy (*24*). After severing in the wild type (Fig. 3, A, D, and E) (movie S3), the peak velocity of the posterior spindle pole was ~40% greater than that of the anterior one, reflecting a larger net pulling force (*5*). Moreover, the posterior spindle pole traveled farther and underwent more extensive transverse oscillations (*5*). After severing in *gpr-1/2*(*RNAi*) embryos (Fig. 3, B, D, and E) (movie S4) (*25*), both spindle poles achieved the same peak velocity after severing, which was much less than that of even the anterior spindle pole in severed wild-type embryos. Moreover, the liberated spindle poles hardly traveled and did not undergo transverse oscillations. We found essentially identical results in *goa-1/gpa-16*(*RNAi*) embryos (Fig. 3, C to E) (movie S5) (*25*). Impaired pulling forces are unlikely to result from defective astral microtubules, because the microtubule network in fixed one-cell stage *gpr-1/2*(*RNAi*) or *goa-1/gpa-16*(*RNAi*) embryos was indistinguishable from that in the wild type (Fig. 4J) (*14*). Thus, Gα signaling is required to generate substantial pulling force on spindle poles during mitosis.

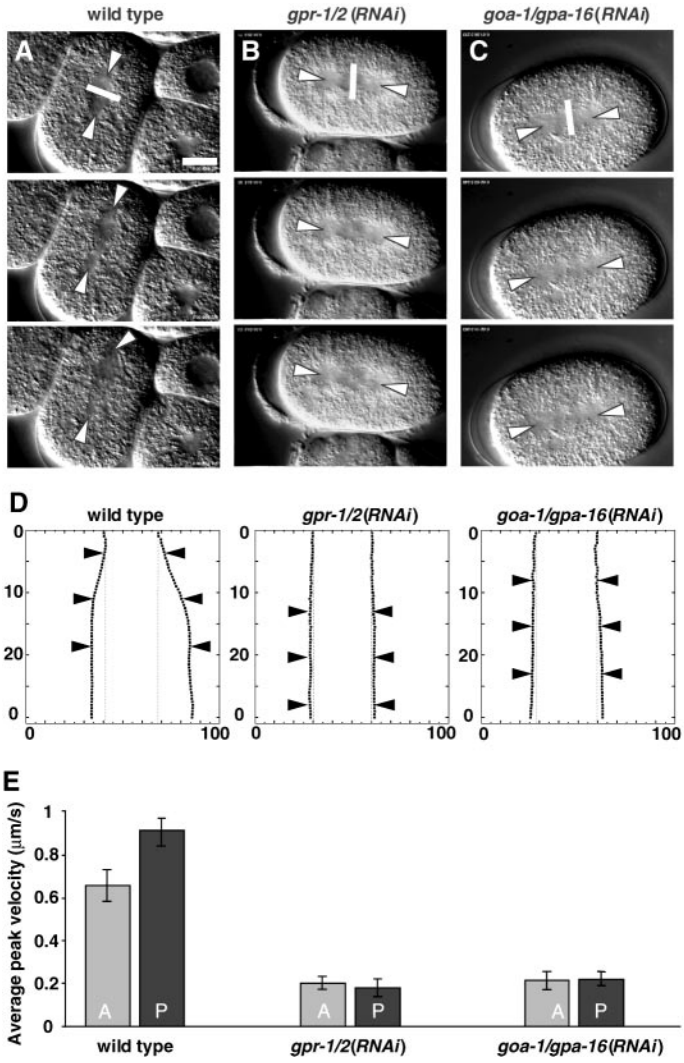

Fig. 3. GPR-1/2, as well as GOA-1 and GPA-16, are required for generation of astral pulling forces. (**A** to **C**) Time-lapse DIC microscopy sequence of spindle-severing experiments in wild-type (A) (anterior is at the lower left), *gpr-1/2*(*RNAi*) (B), or *goa-1/gpa-16*(*RNAi*) (C) one-cell stage embryos. The first frame in each sequence corresponds to the time of the last laser shot (white bar indicates location of cut), the second frame is 7.5 s later, the third frame 7.5 s thereafter. All panels are at same magnification; scale bar, 10 μm. (**D**) Tracings of spindle pole position corresponding to sequences shown in (A) to (C). Tracings start at first laser shot (20 s after beginning of movies S3 to S5); arrowheads indicate time points corresponding to frames in (A) to (C). (**E**) Average peak velocities achieved by anterior and posterior spindle poles after severing [wild-type, *n* = 34, values from (*5*); values for *gpr-1/2* (*RNAi*) and *goa-1/gpa-16*(*RNAi*) in (*25*)]. Error bars show SEM at the 0.95 confidence interval.

The spindle-severing experiments raised the possibility that GPR-1/2, as well as GOA-1 and GPA-16, also acted to ensure an imbalance of pulling forces in response to polarity cues, because residual forces in *gpr-1/2*(*RNAi*) or *goa-1/gpa-16*(*RNAi*) embryos were equal on both spindle poles. We investigated whether the distribution of GPR-1/2 may offer an explanation for this observation. Antibodies to a peptide identical in GPR-1 and GPR-2 labeled the cell cortex and the cytoplasm, as well as the vicinity of centrosomes to a lesser extent (Fig. 4, A to H) (fig. S3). All aspects of the

staining pattern were essentially abolished in *gpr-1/2*(*RNAi*) embryos (Fig. 4I). Although the distribution of GPA-16 has not been reported, GOA-1 is present at the cell cortex and the cytoplasm as well as in the vicinity of centrosomes (*6, 26*), which supports the notion that GPR-1/2 function with GOA-1 in vivo.

We analyzed the distribution of GPR-1/2 in detail throughout the cell cycle. Cortical GPR-1/2 were uniform in 67% (n = 60) of prophase one-cell stage embryos (*14*) but slightly asymmetric in 33% of them, with more protein at the posterior cortex (Fig. 4, A and B) (fig. S3). Between the end of prophase and early anaphase, 96% of one-cell stage embryos (n = 24) exhibited an enriched distribution at the posterior cortex (Fig. 4, C and D) (fig. S3). A similar enrichment was also apparent early in the cell cycle in the posterior blastomeres P_1 and P_2 at the two- and four-cell stages, respectively (Fig. 4, E to H). We obtained an identical distribution with antibodies from another rabbit immunized against the same peptide (*14*). To independently assess the distribution of GPR-1 and GPR-2, we generated transgenic animals expressing GPR-2 fused to GFP, which exhibited a distribution similar to that seen with antibodies to GPR-1/2 (Fig. 4, K and L).

Both GPR-1 and GPR-2 lack discernible protein motifs that may target them to the plasma membrane. In contrast, both GOA-1 and GPA-16 harbor N-myristoylation sites, raising the possibility that the presence of GPR-1/2 at the cell cortex occurs through interaction with membrane-tethered Gα subunits. Consistent with this view, the cortical distribution of GPR-1/2 was severely diminished in *goa-1*/*gpa-16*(*RNAi*) embryos [Fig. 4, M and N; average cortical/cytoplasmic signal of 0.92 (SD = 0.30, n = 8) versus 1.75 in the wild type (SD = 0.26, n = 9)].

We used the cortical asymmetry of GPR-1/2 to address whether they act downstream of the PAR proteins or in a parallel pathway. We focused on early two-cell stage embryos in which the enrichment of GPR-1/2 at the posterior cortex was easiest to score and apparent in 81% of the wild-type embryos (n = 57; Fig. 4E). The cortical distribution of GPR-1/2 was uniform in 100% of *par-3* mutant and *par-2*(*RNAi*) early two-cell stage embryos (n = 24 and 17, respectively; Fig. 4, O to R). Moreover, levels at the cell cortex were stronger in *par-3* mutant embryos than in *par-2*(*RNAi*) embryos, as expected because both daughter cells exhibit posterior-like features in the absence of *par-3* function and anterior-like features in the absence of *par-2* function (*3*). Analogous conclusions were reached by examining one-cell stage embryos (*14*). Furthermore, spindle-severing experiments in embryos simultaneously lacking *par-3* function and *gpr-1/2* function revealed that *gpr-1/2* are epistatic to *par-3* for force generation (*25*). Thus, *gpr-1/2* act downstream of AP polarity cues to mediate proper spindle positioning in one-cell stage embryos. *par-2* and *par-3* also control the distribution of the DEP domain–containing protein LET-99 in a posterior cortical belt in one-cell stage embryos (*27*). However, the first cleavage is unequal in *let-99* mutant embryos (*28*), which suggests that *let-99* is not essential for differential force generation during anaphase.

We propose a working model in which AP polarity cues set by the PAR proteins translate into distinct pulling forces on the two spindle poles via differential activation of Gα signaling at the cell cortex (fig. S4). Because there is more GPR-1/2 on the posterior cortex, there is also more Gα signaling, and a larger net pulling force is exerted on the posterior spindle pole. A fluctuation analysis predicts that an imbalance of pulling forces stems from a difference in the number of cortical force generators pulling on astral microtubules, with ~50% more being present on the posterior cortex (*29*). The posterior enrichment of GPR-1/2 is of a similar extent (fig. S3), which suggests that Gα signaling at

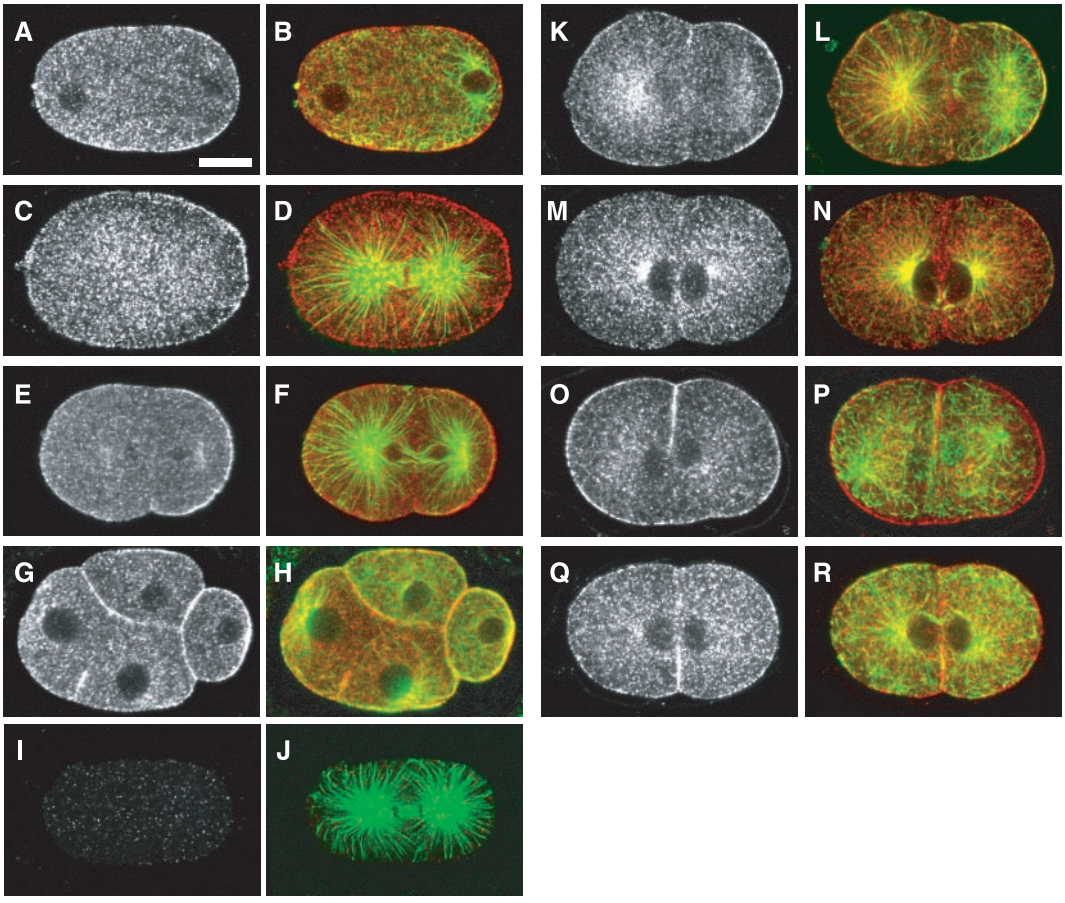

Fig. 4. Cortical distribution of GPR-1/2 is asymmetric and controlled by polarity cues. Fixed embryos from wild-type [(**A** and **B**) early prophase one-cell stage; (**C** and **D**) metaphase one-cell stage; (**E** and **F**) early two-cell stage; (**G** and **H**) early four-cell stage], *gpr-1/2*(*RNAi*) [(**I** and **J**) telophase one-cell stage], and early two-cell stage GFP–GPR-2 (**K** and **L**), *goa-1*/*gpa-16*(*RNAi*) (**M** and **N**), *par-3*(*it71*) (**O** and **P**), and *par-2*(*RNAi*) (**Q** and **R**) stained with antibodies to GPR-1/2 (A to J, M to R) or GFP (K and L) and to α-tubulin (panels in right columns show GPR-1/2 or GFP in red, α-tubulin in green). All panels are at approximately same magnification; scale bar, 10 μm.

the cell cortex is a rate-limiting step for force generator function. Given that cortically localized $G\alpha_i$ and Pins also dictate spindle positioning in *Drosophila* (*10*), we propose that modulation of cortical Gα signaling to generate defined pulling forces on astral microtubules is a conserved mechanism to translate polarity cues into appropriate spindle positioning.

References and Notes

1. J. A. Knoblich, *Nature Rev. Mol. Cell Biol.* **2**, 11 (2001).
2. P. Gönczy, *Trends Cell Biol.* **12**, 332 (2002).
3. J. Pellettieri, G. Seydoux, *Science* **298**, 1946 (2002).
4. K. J. Kemphues, J. R. Priess, D. G. Morton, N. Cheng, *Cell* **52**, 311 (1988).
5. S. W. Grill, P. Gönczy, E. H. Stelzer, A. A. Hyman, *Nature* **409**, 630 (2001).
6. M. Gotta, J. Ahringer, *Nature Cell Biol.* **3**, 297 (2001).
7. F. Yu, X. Morin, Y. Cai, X. Yang, W. Chia, *Cell* **100**, 399 (2000).
8. M. Schaefer, A. Shevchenko, J. A. Knoblich, *Curr. Biol.* **10**, 353 (2000).
9. M. Schaefer, M. Petronczki, D. Dorner, M. Forte, J. A. Knoblich, *Cell* **107**, 183 (2001).
10. Y. Cai, F. Yu, S. Lin, W. Chia, X. Yang, *Cell* **112**, 51 (2003).
11. P. Gönczy *et al.*, *Nature* **408**, 331 (2000).
12. Examination of the genome sequence and sequencing of full-length cDNAs revealed that *gpr-1* (WormBase code F22B7.13) and *gpr-2* (C38C10.4) are both expressed and that they result from a recent gene duplication event. We found a single *gpr* homolog in the available *C. briggsae* genome (CBG10100), whose inactivation caused a phenotype indistinguishable from that observed in *C. elegans*.
13. B. Zhang *et al.*, *Nature* **390**, 477 (1997).
14. K. Colombo, P. Gönczy, unpublished data.
15. B. Etemad-Moghadam, S. Guo, K. J. Kemphues, *Cell* **83**, 743 (1995).
16. L. Boyd, S. Guo, D. Levitan, D. T. Stinchcomb, K. J. Kemphues, *Development* **122**, 3075 (1996).
17. S. Guo, K. J. Kemphues, *Cell* **81**, 611 (1995).
18. T. J. Hung, K. J. Kemphues, *Development* **126**, 127 (1999).
19. S. Strome, W. B. Wood, *Cell* **35**, 15 (1983).
20. K. J. Reese, M. A. Dunn, J. A. Waddle, G. Seydoux, *Mol. Cell* **6**, 445 (2000).
21. L. De Vries *et al.*, *Proc. Natl. Acad. Sci. U.S.A.* **97**, 14364 (2000).
22. R. J. Kimple *et al.*, *J. Biol. Chem.* **276**, 29275 (2001).
23. M. Natochin, K. G. Gasimov, N. O. Artemyev, *Biochemistry* **40**, 5322 (2001).
24. See supporting online material.
25. Average peak velocities in μm/s (±SEM at the 0.95 confidence interval) were as follows (A, anterior spindle pole; P, posterior spindle pole): *gpr-1/2*(*RNAi*), A: 0.20 ± 0.03, P: 0.18 ± 0.04, $n = 15$; *goa-1/gpa-16*(*RNAi*), A: 0.21 ± 0.04, P: 0.22 ± 0.03, $n = 15$; *par-3*(*it71*) *gpr-1/2*(*RNAi*), A: 0.18 ± 0.04, P: 0.18 ± 0.03, $n = 13$. Values for *par-3*(*it71*) were A: 0.89 ± 0.11, P: 0.90 ± 0.07, $n = 20$ (*5*).
26. K. G. Miller, J. B. Rand, *Genetics* **156**, 1649 (2000).
27. M. F. Tsou, A. Hayashi, L. R. DeBella, G. McGrath, L. S. Rose, *Development* **129**, 4469 (2002).
28. L. S. Rose, K. Kemphues, *Development* **125**, 1337 (1998).
29. S. W. Grill, J. Howard, E. Schäffer, E. H. K. Stelzer, A. A. Hyman, unpublished data.

30. We thank A. Ashford, J. Corbitt, T. K. Harden, M. Glozter, A. Hyman, M. Koelle, Y. Kohara, G. Seydoux, and V. Simanis for reagents; A. Debant and S. Schmidt for advice; K. Baumer for technical support; M. Brauchle for movie S1; and K. Afshar, M. Delattre, and M. Labouesse for critical reading of the manuscript. Supported by Swiss National Science Foundation grant 31-62102.00 (P.G.) and NIH grant GM62338 (D.P.S.).

Supporting Online Material

www.sciencemag.org/cgi/content/full/1084146/DC1
Materials and Methods
Figs. S1 to S4
References
Movies S1 to S7

28 February 2003; accepted 8 May 2003
Published online 15 May 2003;
10.1126/science.1084146
Include this information when citing this paper.

Transmission Dynamics of the Etiological Agent of SARS in Hong Kong: Impact of Public Health Interventions

Steven Riley,[1]*† Christophe Fraser,[1]* Christl A. Donnelly,[1] Azra C. Ghani,[1] Laith J. Abu-Raddad,[1] Anthony J. Hedley,[2] Gabriel M. Leung,[2] Lai-Ming Ho,[2] Tai-Hing Lam,[2] Thuan Q. Thach,[2] Patsy Chau,[2] King-Pan Chan,[2] Su-Vui Lo,[3] Pak-Yin Leung,[4] Thomas Tsang,[4] William Ho,[5] Koon-Hung Lee,[5] Edith M. C. Lau,[6] Neil M. Ferguson,[1] Roy M. Anderson[1]

We present an analysis of the first 10 weeks of the severe acute respiratory syndrome (SARS) epidemic in Hong Kong. The epidemic to date has been characterized by two large clusters—initiated by two separate "super-spread" events (SSEs)—and by ongoing community transmission. By fitting a stochastic model to data on 1512 cases, including these clusters, we show that the etiological agent of SARS is moderately transmissible. Excluding SSEs, we estimate that 2.7 secondary infections were generated per case on average at the start of the epidemic, with a substantial contribution from hospital transmission. Transmission rates fell during the epidemic, primarily as a result of reductions in population contact rates and improved hospital infection control, but also because of more rapid hospital attendance by symptomatic individuals. As a result, the epidemic is now in decline, although continued vigilance is necessary for this to be maintained. Restrictions on longer range population movement are shown to be a potentially useful additional control measure in some contexts. We estimate that most currently infected persons are now hospitalized, which highlights the importance of control of nosocomial transmission.

The evolution and spread of the etiological agent of severe acute respiratory syndrome (SARS), a novel coronavirus (*1*), has resulted in an unparalleled international effort coordinated by the World Health Organization (WHO) to characterize the virus, develop diagnostic tests, and formulate optimal treatment protocols to reduce morbidity and mortality (*2–4*). Great progress has been made with, for example, the full sequence of the RNA virus reported on 13 April 2003 (*5, 6*). The epidemic apparently originated in early November in the Guandong province of the People's Republic of China, and then spread rapidly throughout the world via air travel. As of 21 May 2003, 7956 cases have been reported to WHO from 28 countries, with 666 deaths recorded. The epidemics in Hong Kong, mainland China, Singapore, Taiwan, and Toronto (Canada) have been of particular concern because of the multiple generations of local transmission seen in those areas. The extent of these epidemics has been worsened by the occurrence of large clusters of infection linked to single individuals and/or spatial locations.

The rate of spread of an epidemic—and whether such spread is self-sustaining—depends on the magnitude of a key epidemiological parameter, the basic reproduction number (R_0), defined as the average number of secondary cases generated by one primary case in a susceptible population (*7*). After the introduction of an agent into a population, a

[1]Department of Infectious Disease Epidemiology, Faculty of Medicine, Imperial College London, Exhibition Road, London SW7 2AZ, UK. [2]Department of Community Medicine, University of Hong Kong, 21 Sassoon Road, Pokfulam, Hong Kong. [3]Research Office, Health, Welfare and Food Bureau, Government of the Hong Kong Special Administrative Region, 19th Floor, Murray Building, Garden Road, Hong Kong. [4]Department of Health, Government of the Hong Kong Special Administrative Region, Wu Chung House, 213 Queen's Road East, Wanchai, Hong Kong. [5]Hong Kong Hospital Authority, 147B Argyle Street, Kowloon, Hong Kong. [6]Department of Community and Family Medicine, Chinese University of Hong Kong, School of Public Health, Prince of Wales Hospital, Shatin, N.T., Hong Kong.

*These authors contributed equally to this work.
†To whom correspondence should be addressed. E-mail: s.riley@imperial.ac.uk